

Acrylamide-plasma treated electrospun polystyrene nanofibrous adsorbents for cadmium and nickel ions removal from aqueous solutions

Alireza Bahramzadeh,¹ Payam Zahedi,¹ Majid Abdouss²

¹School of Chemical Engineering, College of Engineering, University of Tehran, Tehran, Iran

²Department of Chemistry, Amirkabir University of Technology (Tehran Polytechnic), Tehran, Iran

Correspondence to: P. Zahedi (E-mail: phdzahedi@ut.ac.ir)

ABSTRACT: The aim of this work was to prepare novel electrospun polystyrene (PS) nanofibrous samples functionalization with acrylamide monomer (AAM) as promising nanoadsorbents by the use of nitrogen gas plasma. To investigate the performance evaluation of the samples for adsorbing cadmium (Cd^{2+}) and nickel (Ni^{2+}) ions, a series of tests in terms of ATR-FTIR spectroscopy, FE-SEM, water contact angle (WCA) measurements and atomic adsorption spectroscopy were carried out. The ATR-FTIR results showed that nitrogen (N_2) plasma was an efficient tool because of the formation of functionalized AAM-PS nanofibrous samples by providing amide ($-\text{NCO}$) and amine ($-\text{NH}-$) groups onto their surfaces. The WCA measurements demonstrated that the N_2 plasma-modified samples in the presence of AAM had a lower contact angle of 42.8° than the other samples. Moreover, FE-SEM micrograph images of AAM-treated PS nanofibrous samples indicated that appropriate amount of the functional groups onto the samples surfaces were deposited. Afterwards, AAS analysis along with Langmuir and Freundlich's isotherm models revealed that a high adsorption of the ions was occurred at pH 5 in the order Cd^{2+} (10 mg g^{-1}) > Ni^{2+} (4.9 mg g^{-1}) by using the nanoadsorbents dosage 1 g L^{-1} and the metal ions concentration 25 mg L^{-1} . In addition, the obtained results exhibited the Cd^{2+} and Ni^{2+} ions removal efficiencies (%R) were increased up to 96% and 94%, respectively with raising the nanoadsorbents dosage. Moreover, the equilibrium adsorption of the ions showed the best fitting by the Freundlich's model. Finally, the desorption of the optimized samples for regenerating them owing to the effective removal of the ions has been confirmed by applying the recyclability test. © 2015 Wiley Periodicals, Inc. *J. Appl. Polym. Sci.* **2016**, *133*, 42944.

KEYWORDS: adsorption; electrospinning; polystyrene

Received 7 June 2015; accepted 15 September 2015

DOI: 10.1002/app.42944

INTRODUCTION

Over the past few years, heavy metals pollution has received a considerable attention issue owing to its environmental problem, which required immediate and urgent action. Some heavy metals such as nickel (Ni^{2+}) and cadmium (Cd^{2+}) are highly toxic even in lower concentrations from 0.001 to 0.1 mg mL^{-1} in water or other aquatic life for people's health and agriculture.^{1,2}

There are several methods to remove heavy metal ions from aqueous solutions including adsorption,^{3,4} ion exchange, chemical oxidation, reverse osmosis and so forth.^{5–10} Among these processes, adsorption has several advantages compared to other techniques because of high removal efficiency, ease of operation, simplicity of design, low initial cost, and insensitivity of toxic substances.^{11,12} These advantages have made it the most economical and effective treatment method for the removal of the substances such as dyes¹³ and copper.¹⁴ For increasing adsorption efficiency, surface modifications of synthetic and semi-natural polymers by using a

few functional groups in terms of carboxylic, sulfonic, amide, and amine have been abundantly developed.^{15–22}

Although PS has widely appropriate characteristics such as good mechanical properties and chemical resistance, ease of electrospinning, and low cost, it cannot individually adsorb metal ions efficiently. Bulbul-Sonmez *et al.*²³ investigated polyacrylamide (PAAm) functionalized-crosslinked PS beads by the use of atom transfer radical polymerization technique and applied for mercury (Hg^{2+}) ion removal from the solution. Also, Reddy *et al.*²⁴ prepared PS-supported chelating polymer resins functionalized with four active reagent groups in terms of glycine, hydroxyl benzoic acid, Schiff base, and diethanol amine and evaluated their performance at pH 10 and pH 6 for chrome (Cr^{5+}), Cd^{2+} as well as Hg^{2+} and (lead) Pb^{2+} metal ions removal. They concluded that the resins were more selective at pH 10 for Pb^{2+} and Hg^{2+} , whereas at pH 6 they found to be Cr^{5+} and Cd^{2+} selective. Recently, Masoumi and coworkers²⁵ reported the

structural modification of acrylonitrile–butadiene–styrene waste as an efficient nanoadsorbent for a series of heavy metal ions removal including Pb^{2+} , Cu^{2+} , Cd^{2+} , and zinc (Zn^{2+}) from water. They have resulted in the removal efficiency (%R) for Pb^{2+} , Cu^{2+} , Zn^{2+} , and Cd^{2+} were 90.8%, 89.6%, 84.5%, and 82%, respectively at pH 6. Moreover, Saadeh *et al.*²⁶ synthesized a new PS-based terpyridine polymer for the adsorption of Ni^{2+} , Cu^{2+} , Pb^{2+} , and Zn^{2+} ions. Their study showed that the maximum equilibrium capacity of the ions in the order mentioned above were about of 10, 75, 80, and 40 mg g^{-1} at pH 7 during 25 min, respectively.

Currently, electrospun polymeric nanofibers are being received a great deal of attention used for nanoadsorbents because of their unique properties such as porous structures, high specific surface areas, suitable adsorption kinetics, lower pressure drop, flexible component adjustment, high permeation flux, and even multitarget adsorption as well as low cost, which have made them favorable for waste water treatment and purification.^{20,27,28} Electrospinning is a promising fibers forming technique for the production of long nanofibers with diameters in the range of nanometers to a few microns.²⁹ So far, a limited research works regarding the use of either nanofibers membranes or their functionalized surfaces for heavy metal ions removal from aqueous solutions have been published. For example, Feng *et al.*³⁰ have done a comparison between electrospun PS and styrene–butadiene–styrene (SBS)/PS blend nanofibers for copper ion (Cu^{2+}) adsorption. The electrospun samples have been treated with sulphuric acid owing to their surface modification via sulfonic groups before adsorption. They showed that PS/SBS blend nanofibrous samples have more rapid adsorption rate for Cu^{2+} than that of those samples consisted of pure PS because there were more exposed functional groups for the metal ion onto the surface of the samples. Furthermore, a similar procedure regarding removal of different heavy metal ions including Cu^{2+} , Pb^{2+} , and Cr^{6+} by using an electrospun chitosan/graphene oxide composite nanofibrous adsorbent was carried out by Najafabadi and coworkers.³¹

There are many techniques that can be used to alter polymers surfaces properties such as laser,³² plasma,³³ and corona discharge,³⁴ nevertheless there has been growing interest in applying plasma through surface functionalizing followed by its modification. In this technique the consumption of chemicals is low, and hence the requirements for their disposal and any other by products are minimal.^{35,36} The interaction of a nitrogen-containing plasma (N_2 plasma) with a polymer surface leads to nitration introduces in different functional groups onto the polymer surface. However, N_2 plasma can introduce nitrogen functions such as amine, mostly primary amine (NH_2), imine ($\text{CH}=\text{NH}$), cyano ($-\text{CN}$), and nitrile³⁷ and makes an activated polymer surface for further functionalization process. For the first time, Paynter³⁸ modified the PS surface via N_2 and N_2/H_2 plasmas in order to deposit oxygen and nitrogen groups onto the polymer surface. The X-ray photoelectron spectroscopy results revealed the presence of binding energies of the N_{1s} and O_{1s} photoelectron onto the PS surface after plasma treatment. Moreover, Boulares-Pender *et al.*³⁹ investigated N_2 plasma in order to functionalize amine group onto the PS surfaces in

which an appropriate modification for the immobilization of some biological compounds was achieved. Also, Chan *et al.*⁴⁰ reported a successful primary amino group's deposition onto PS surfaces by treating with ammonia plasma (NH_3 plasma).

It should be noted that in the above reports, the performance evaluation of electrospun PS nanofibers for heavy metal ions removal has not been considered and neither their N_2 plasma functionalization followed by AAm treatment nor isotherm adsorption models investigation have been ever carried out so far. Furthermore, by studying the all reported literature, two following significant points can be concluded: (1) a merely investigation on removal of Cd^{2+} and Ni^{2+} ions from aqueous solutions has been carried out by using PS nanofibrous adsorbents and (2) the various modification techniques reported on PS have not an efficient performance in order to remove those heavy metal ions especially Ni^{2+} from water remarkably.

The objective of this work was to prepare acrylamide-functionalized electrospun PS nanofibrous samples by means of N_2 , N_2/H_2 , and NH_3 plasmas and to evaluate their amount functionalizing level by using ATR-FTIR and FE-SEM as well as WCA measurements. Afterwards, the adsorption studies of the optimized functionalized nanofibrous sample related to Cd^{2+} and Ni^{2+} ions as functions of pH and nanoadsorbent dosage along with Freundlich and Langmuir's equations as isotherm adsorption models by the use of AAS were carried out. Finally, the recyclability of the optimized sample for the desorption and capacity for removal of the ions from aqueous solutions was investigated.

EXPERIMENTAL PROCEDURE

Preparation of PS Nanofibrous Samples via Electrospinning

The weighed 2 g of PS granules (grade ST316310, weight average molecular weight of 70 kDa, provided from Goodfellow Cambridge, Huntingdon, United Kingdom) were dissolved in 7 mL chloroform and stirred for about 2 h at room temperature. Then 3 mL dimethylformamide (DMF) were added to the solution and finally mixed for 30 min. The solution was transferred to a syringe for electrospinning process. All the chemicals were analytical reagent grades and used without further purification.

The electrospinning device was a model eSpinner NF-CO EN/II (Asian Nanostructures Technology, Tehran, Iran). The electrospinning conditions for the preparation of the optimized PS nanofibrous samples with a minimum average diameter were obtained by Motealleh *et al.*⁴¹ and listed as follows: solution flow rate = 0.6 mL h^{-1} , applied voltage = 18 kV and the distance between the syringe needle tip and the collector = 15.5 cm. The nanofibrous samples were electrospun for 2 h and collected on a sterile aluminum foil. To ensure the organic solvents evaporation from the spun fibers, the samples were dried at ambient temperature for about 12 h until a constant weight was attained.

Surface Modification of the Nanofibrous Samples via Different Gas Plasmas

Four different plasma-modified nanofibrous samples were prepared as follows: (1) plasma modification in the presence of N_2 gas environment (sample A), (2) plasma modification in the presence of N_2 and H_2 gases mixture (N_2/H_2 ratio of 2.2) (sample B), (3) plasma modification in the presence of NH_3 gas environment

Table I. Different Plasma-Modification Recipes of the Electrospun PS Nanofibrous Samples

Sample	Gas flow rate (sccm) ^a	Plasma operation time (s)
A ₁	220 sccm N ₂	90
A ₂	220 sccm N ₂	180
B ₁	220 sccm N ₂ +100 sccm H ₂	90
B ₂	220 sccm N ₂ +100 sccm H ₂	180
C ₁	220 sccm NH ₃	90
C ₂	220 sccm NH ₃	180
D ₁	220 sccm N ₂ +functionalization with AAm	90
D ₂	220 sccm N ₂ +functionalization with AAm	180

^aStandard cubic centimeters per minute

(sample C), and (4) plasma modification in the presence of N₂ gas followed by functionalizing with AAm (density of 1.127 g cm⁻³, molecular weight of 71.07 Da and melting point of 84°C, purchased from Merck, Germany) (sample D). These samples were treated with low-pressure plasma in a RF generator in PECVD chamber (LPCVD, 790 Unaxis, University of Texas at Dallas) at four different plasma conditions below: operation power 100 W, frequency 13.56 MHz, pressure 1000 mTorr, and temperature 21°C. Table I shows the various characteristics of the samples provided by using different gases plasmas either 90 s or 3 min. To prevent cross-linking or degradation reactions of the samples surfaces, the lowest operational power of the plasma process was applied.⁴² In contrast to the preparation of the samples (A), (B), and (C), the sample (D) has a different modification procedure which was first irradiated by plasma during time of 90s [sample (D₁)] and 3 min [sample (D₂)] and then they were immediately immersed into the AAm solution [30 (%w/v) AAm in distilled water] for about 3 h. After functionalizing, the probably provided residual monomers and homopolymers were removed from the surfaces of the nanofibrous samples by washing in distilled water for about 30 min. It was assumed that the whole residues from the samples surfaces were easily removed by the use of distilled water washing because of a remarkable difference between the contact angles of the AAm and PS nanofibers. In other words, the AAm was neither adsorbed nor preadsorbed onto the nanofibers surfaces.⁴³

Characterizations of the Plasma-Modified Samples

Attenuated Total Reflectance Fourier Transformed Infrared Spectroscopy. An attenuated total reflectance Fourier transformed infrared (ATR-FTIR) spectroscopy analysis (Bruker model EQUINOX 55, United States, with a resolution of 4 cm⁻¹) was applied in order to determine functionalizing either amine or acrylamide groups onto the surfaces of four samples (A–D) treated by plasmas including N₂, N₂/H₂, NH₃, and also N₂/AAm solution at 90 s and 3 min and the ATR-FTIR results were compared to the sample without plasma-treatment. The scan process was carried out from 4000 cm⁻¹ (2.5 μm in thickness) to 650 cm⁻¹ (15.4 μm in thickness). To

achieve a more precision in the obtained spectrum, an average of 16 scans was recorded.

Functionalization or Grafting Yield Determination. One of the main criteria regarding the suitability of the functionalizing process is an increasing observation regarding the weight of the electrospun PS nanofibrous samples after AAm functionalization compared to those samples without the functionalization. The functionalizing yield was calculated according to the following equation:

$$\text{G.Y. (\%)} = [(W_1 - W_2) / W_1] \times 100, \quad (1)$$

where “W₁” and “W₂” are the weights of the PS nanofibrous samples before and after AAm functionalizing, respectively.⁴⁴

Water Contact Angle Measurements. The water contact angles (WCA) of un-treated and plasma-treated electrospun PS nanofibrous samples were determined with a G10 contact goniometer (Kruss, Germany) by using doubly deionized water (DDI) as wetting liquid at 25°C with a relative humidity of about 32 ± 1%. To ensure the valuable measurements, both Teflon (PTFE) and glass (standard hydrophobic and hydrophilic materials) were used. For calculating the average contact angles of the samples with *P*-value < 0.05, 10 data points of water drops for the each sample were recorded.

Field Emission Scanning Electron Microscopy Studies. The electrospun nanofibrous samples were coated with a thin layer of gold by Bio-Rad E5200 auto sputter coater (United Kingdom). For morphological observations of the samples a field emission scanning electron microscope (FE-SEM; Hitachi model S4160, Japan) with 3000× and 10,000× magnifications was utilized. The mean values of the nanofibers diameters from 10 different sections were measured via ImageJ software and recorded.

Adsorption Equilibrium Experiments of the Optimized Sample along with the Recyclability Studies. The adsorption equilibrium studies of the optimized plasma-treated electrospun PS nanofibrous sample functionalization with AAm which was denoted by [sample (D₂)], were carried out as a batch-wise process. The heavy metal ions solutions were made by the use of the hydrated nickel sulphate (NiSO₄·6H₂O) and the hydrated cadmium sulphate (CdSO₄·8H₂O) were separately dissolved in distilled water with the initial ion concentration of 25 mg L⁻¹. First, in order to determine the effective pH of these prepared ions solutions because of determining the maximum equilibrium adsorption of Ni²⁺ and Cd²⁺ ions via the sample (D₂) as the nano-adsorbent, the weighed 0.4 g nanofibrous sample was added to the 450 mL of the each metal ions solutions separately in different pHs ranging from 2 to 6 at room temperature (~23°C) during 2 h period. The impact of the nano-adsorbent concentrations in order to remove the heavy metal ions from the prepared solutions was also investigated. For this purpose, the sample in the amounts of ranging from 0.2 to 2 g were immersed into the 450 mL solutions of Ni²⁺ and Cd²⁺ ions with 25 mg L⁻¹ concentration at pH 5 and temperature 23°C during time 2 h. The adsorption of the optimized sample for removing the ions from the aqueous was determined by AAS (model PU910, Philips, Amsterdam, The Netherlands). Generally, the amount of adsorbate (mg g⁻¹) was calculated using the formulae reported by Vanderborght and Van Grieken⁴⁵ as follows:

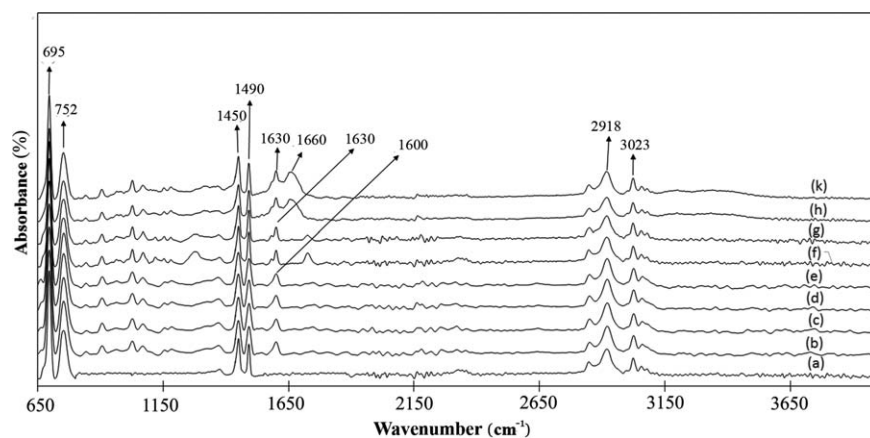


Figure 1. FTIR spectrum of PS nanofibrous samples: (a) without plasma treatment, (b) treated with N_2 plasma for 90 s, (c) treated with N_2 plasma for 3 min, (d) treated with N_2/H_2 (2.2 ratio) for 90 s, (e) treated with N_2/H_2 (2.2 ratio) for 3 min, (f) treated with NH_3 plasma for 90 s, (g) treated with NH_3 plasma for 3 min, (h) treated with N_2 plasma for 90 s followed by AAm functionalizing and (k) treated with N_2 plasma for 3 min followed by AAm functionalization.

$$q = \frac{V(C_i - C_e)}{W}, \quad (2)$$

where “ q ” is the amount of solute adsorbed from the solution, “ V ” is volume of the adsorbate; “ C_i ” and “ C_e ” are the initial concentration of ions solution before adsorption and the ions solution concentration after adsorption, respectively. At last, “ W ” is the weight (g) of the adsorbent. Also, the removal efficiency (%R) was determined by computing the percentage sorption using the equation below:

$$\text{Sorption}(\%R) = \frac{C_i - C_e}{C_i} \times 100, \quad (3)$$

Furthermore, the performance evaluation of presenting binding sites onto the sample surface with respect to the ions adsorption amounts, was studied by two prominent isotherm adsorption models so-called Langmuir and Freundlich, the following equations, respectively.

$$q_e = \frac{q_m K_L C_e}{1 + K_L C_e} \quad (4)$$

$$q_e = K_F C_e^{\frac{1}{n}} \quad (5)$$

where “ q_m ” ($mg\ g^{-1}$) and “ K_L ” ($L\ mg^{-1}$) are constants in Langmuir’s equation which are referred to the maximum adsorption capacity and the adsorption energy, respectively.⁴⁶ Also, “ q_e ” and “ C_e ” parameters represent the equilibrium adsorption capacity and the equilibrium concentration, respectively. On the other hand, “ K_F ” is the Freundlich’s constant ($mg^{(1-\frac{1}{n})} L^{\frac{1}{n}} g^{-1}$) and “ n ” is a dimensionless number in this model.⁴⁷

Moreover, the desorption capability of the optimized sample because of its regeneration and reuse for the removal of heavy metal ions from aqueous was studied by applying recyclability assay. For this investigation, the sample was recycled three times after absorbing the Ni^{2+} and Cd^{2+} ions by immersing into 50 mL of hydrochloride acid (HCL) with 0.1M solution concentration for 4 h and then after drying the sample completely, it is reused for the ions adsorption with the same conditions.

RESULTS AND DISCUSSION

Characterizations of the AAm-Functionalized Electrospun PS Nanofibrous Sample

ATR-FTIR Analysis. Figure 1 shows the ATR-FTIR spectra of the samples with the following codes: (a) the un-treated electrospun PS nanofibrous sample and the spectra of (b), (c), (d), (e), (f), (g), (h), and (k) corresponding to the samples were denoted by (A_1), (A_2), (B_1), (B_2), (C_1), (C_2), (D_1), and (D_2), respectively which are preliminary represented in Table I. As it can be seen from Figure 1(a), the main characteristic peaks were located at 695, 752, 1450, and 1490 cm^{-1} corresponding to the alkyl groups (e.g., $-CH_2-$ and $-CH-$) in stretching or vibrational frequencies and also the characteristic peaks between wavenumbers of 2918 and 3023 cm^{-1} corresponding to the phenyl group ($-C_6H_5$) through the PS chain backbone. The N_2 plasma-treated samples spectra for 90 s and 3 min are shown in Figure 1(b,c). A similar FTIR spectra were also observed for the samples treated with the mixture of N_2/H_2 plasma as shown in Figure 1(d,e). As it can be concluded from these Figures, the plasmas treatments in the presence of the N_2 and mixed N_2/H_2 (2.2 ratio) gases were enabled to provide cyano group ($-CN-$) at the wavenumber of 1600 cm^{-1} onto the surfaces of the electrospun PS nanofibers. In contrast to aforementioned plasmas, different results were obtained from the NH_3 plasma-modified samples [Figure 1(f,g)] as well as the N_2 plasma-modified samples functionalization with AAm [Figure 1(h,k)]. As it is evident from Figure 1(f,g), a few amine groups were formed and located at 1660 cm^{-1} wavenumber with a medium signal size peak. According to Chan *et al.*⁴⁰ report, NH_3 plasma can create amine groups more suitable than that of N_2 gas plasma onto a polymer surface without any further modification. It can be related to the inherent properties of NH_3 gas compared to N_2 gas. Although NH_3 gas plasma is strongly capable to create higher amounts of radicals onto the surfaces of the polymer materials, simultaneously, a large number of radicals tend to convert other inappropriate functional groups. On the other hand, N_2 plasma has a capability for providing some amounts of radicals less than NH_3 plasma, it can maintain the radicals formed onto the

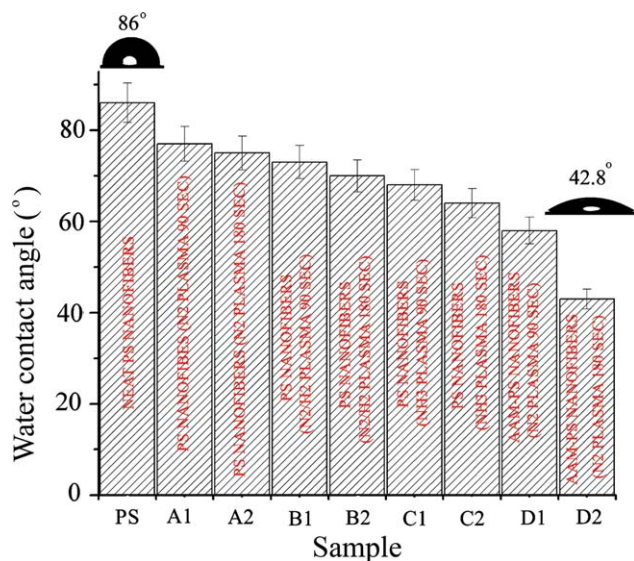


Figure 2. Contact angles of the modified PS nanofibers samples according to the Table I. [Color figure can be viewed in the online issue, which is available at wileyonlinelibrary.com.]

surfaces of the polymer materials without changing them during the further functionalizing process. Therefore, we used N₂ plasma for the modification of the samples were denoted by (D) index followed by functionalizing AAm onto their surfaces. On the basis of Figure 1(h,k), a bimodal peak with small and medium sizes corresponding to the amine and amide functional groups were occurred, respectively.

WCA Measurements and Functionalization Yielding Studies. For increasing the adsorption efficiency of the electrospun nanofibrous samples, an increase in their hydrophilic properties because of the higher performance in adsorbing the heavy metal ions from aqueous solutions is essential. By comparing the contact angles results of the samples in Figure 2, it can be concluded that the sample (D₂) has much more hydrophilic property (WCA = 42.8°) compared to the other samples. Furthermore, the WCA of the neat electrospun PS nanofibers was 86° which was near the WCA of an atactic PS (~85°).⁴⁰ The resulting WCA led to the PS used in this work has also the atactic stereochemistry. A similar study was carried out by Zhao and Geuskens⁴⁸ for evaluating the WCA of AAm-grafted PS, which was confirmed by the obtained WCA of the prepared samples in this work. They showed that a reduction in the contact angles from 80° to 40° was occurred for the neat atactic PS sample and the AAm-grafted PS sample, respectively during hydroxylation time about of 30 min. According to their results, it can be concluded that by deducing the treatment time of N₂ plasma process from 30 to 3 min, a similar results for WCA amounts was achieved as far as the same hydrophilic properties for the samples were attained. Moreover, the functionalizing yields of the sample (D₂) and the sample (D₁) were 16.62 ± 0.2 and 14.20 ± 0.2, respectively, which were also confirmed the WCA measurements. Consequently, the amounts of AAm-functionalized onto the surface of sample (D₂) were about 17% higher than that of the AAm-functionalized onto the surface of sample (D₁).

FE-SEM Observations. Figure 3 (a-d) demonstrates the FE-SEM micrograph images of un-treated electrospun PS nanofibrous sample [Figure 3(a,b)] and the plasma-modified AAm-functionalized

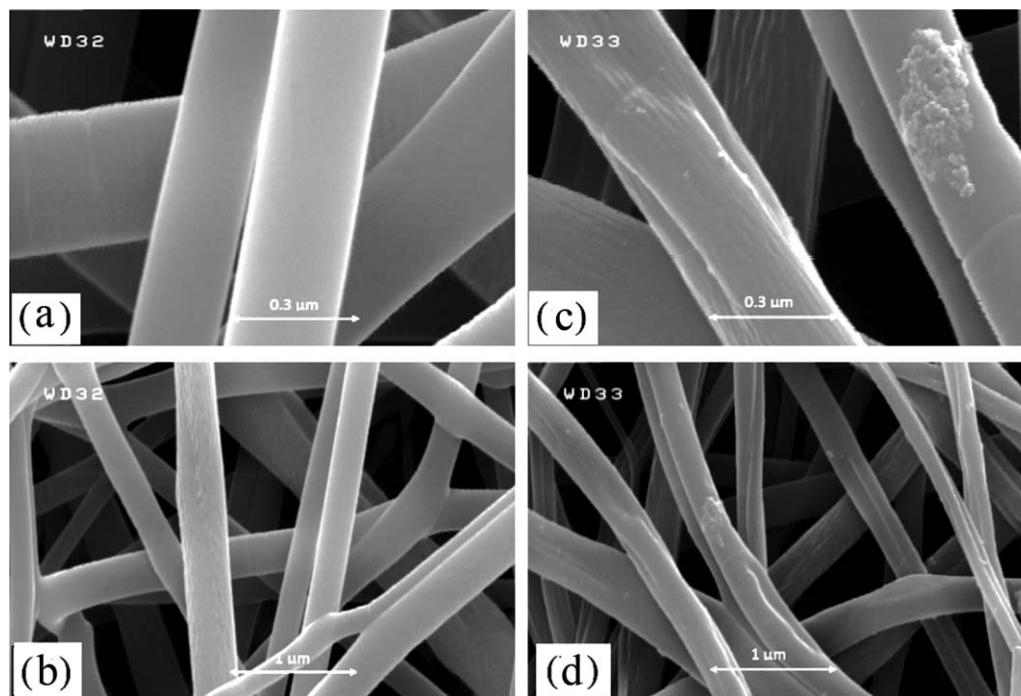


Figure 3. FE-SEM micrograph images of neat PS nanofibers with (a) 10000× magnification, (c) 3000× magnification and the modified PS nanofibers (sample D₂) with (b) 10,000× magnification, (d) 3000× magnification. (The scale bars are 0.3 and 1 microns).

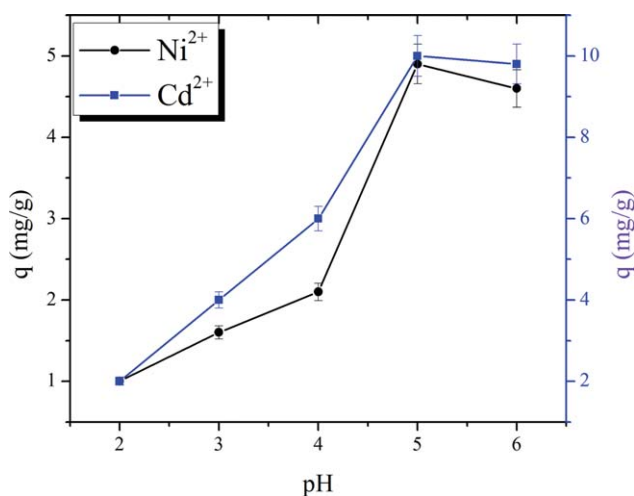


Figure 4. Ion adsorption capacity of modified PS nanofibers versus pH for Cd²⁺ and Ni²⁺ ions. [Color figure can be viewed in the online issue, which is available at wileyonlinelibrary.com.]

PS nanofibrous sample denoted by [sample (D₂)] [Figure 3(c,d)] with two magnifications of 10,000× [Figure 3(a,c)] and 3000× [Figure 3(b,d)]. By observing these morphologies, it can be

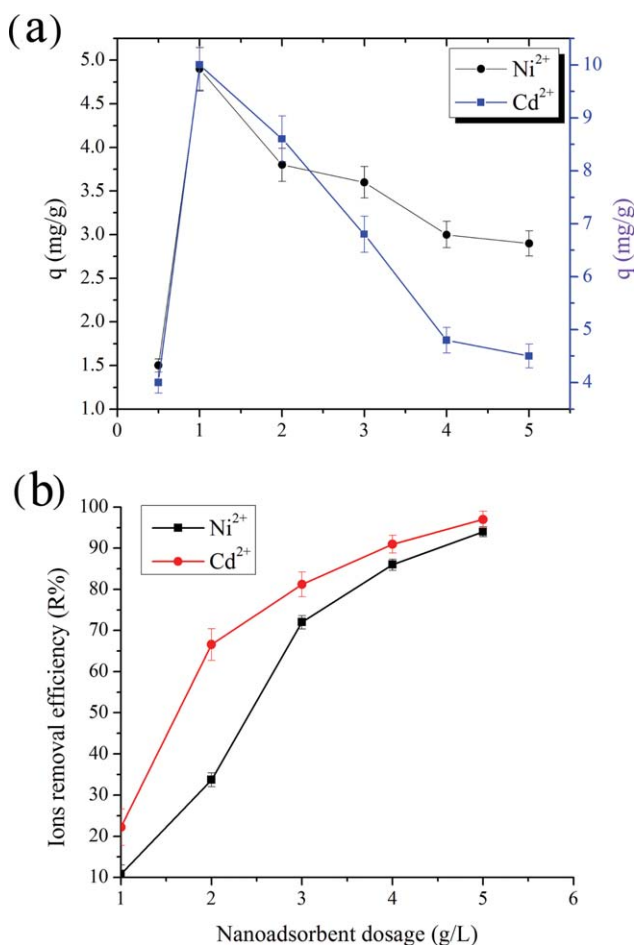
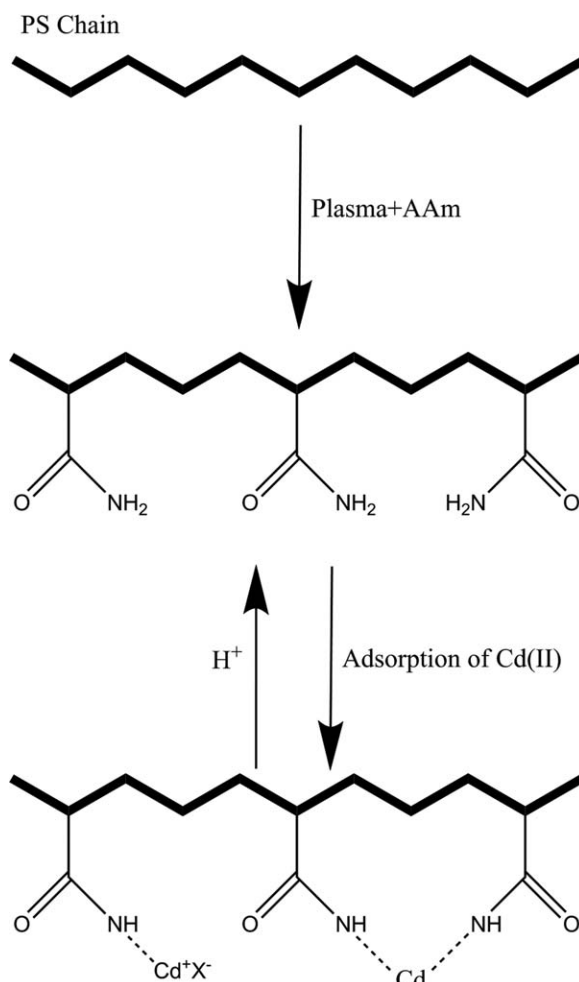


Figure 5. (a) Ion adsorption capacity of modified PS nanofibers versus the nanoadsorbent dosage and (b) ions removal percentage as a function of the nanoadsorbent dosage. [Color figure can be viewed in the online issue, which is available at wileyonlinelibrary.com.]



Scheme 1. A simple schematic of functionalizing AAm monomer onto the PS nanofibers and adsorption mechanisms of Cd²⁺ as a heavy metal ion.

resulted in the neat electrospun PS nanofibrous sample during the optimum conditions of the electrospinning process had a uniform and smooth fibers without beads with an average nanofibers diameter of 247 ± 4 nm [Figure 3(a,b)]. On the other hand, the nanofibers morphology of the N₂ plasma-modified electrospun PS nanofibrous sample functionalization with AAm had a nonuniform and rough fibers along with depositing AAm in the shape of agglomerated particles onto the sample surface with a mean nanofibers diameter of 269 ± 6 nm [Figure 3(c,d)]. The reason for increasing the average nanofibers diameters after functionalization process was referred to the presence of such AAm particles somewhat leading to the nanofibers diameters increase. However, the obtained results revealed the plasma treatment had no significant effect on changing in diameter size of the nanofibrous samples as a nanoadsorbent and hence the sample (D₂) was selected for further evaluation.

Adsorption Equilibrium of Cd²⁺/Ni²⁺ via the Optimized Sample as the Nanoadsorbent and Recyclability Studies

To determine the optimum pH owing to the maximum adsorption of Cd²⁺ and Ni²⁺ ions onto the surface of N₂ plasma-modified electrospun PS nanofibrous sample functionalization with AAm [sample (D₂)], this sample was added to the each

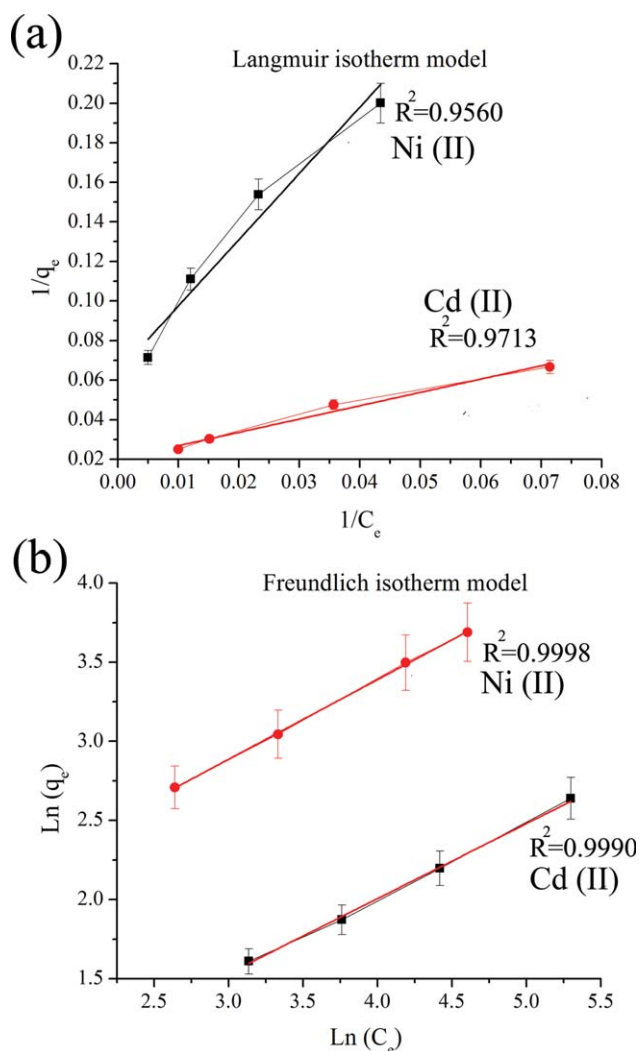


Figure 6. Curve fitting the adsorption data to the (a) Langmuir isotherm and (b) Freundlich's isotherm models. [Color figure can be viewed in the online issue, which is available at wileyonlinelibrary.com.]

metal ions solutions at different pH in the range of 2–6 for 2 h. As reported in the literature,³⁰ a maximum ions adsorption should be attained at pH ranging from 3 to 5. Figure 4 shows the ions adsorption behaviors by using the nanoadsorbent (sample D₂) which resulted in a higher amounts of Cd²⁺ and Ni²⁺ adsorptions about 10 and 4.9 (mg g⁻¹), respectively, at pH 5. At low pH, because of a competitive removal trend between H⁺ and heavy metal ions for producing chelating fibers containing amine as functional groups, a decrease in capability of the nanoadsorbent for attracting the heavy metal ions was occurred. With increasing pH values, the level of positive electric charge through some functionalized active sites onto fibers surface was decreased and led to the metal ions transportation to the surface of the fibers.⁴⁹ The results regarding the ions attachment were related to some factors such as the van der Waals force, chemical and nonchemical bonds and in particular the formation of metal complexes through chelating or ion exchanges.⁵⁰ Figure 5(a,b) illustrates the ions adsorption capacity (q) and the metal ions removal efficiency (%R) of the nanoadsorbent, respectively as a function of the nanoadsorb-

Table II. Linear Langmuir and Freundlich's Isotherm Adsorption Models Parameters and Their Regression Data for Cd²⁺ and Ni²⁺ Ions by Using AAm-Functionalized PS Nanofibers via N₂ Plasma

Isotherm model	Variable	Cd ²⁺	Ni ²⁺
Freundlich	K_F	3.9582	1.0936
	n	1.986	2.087
	R^2	0.9990	0.9998
Langmuir	K_L	0.03	0.02
	q_m	49.5	15.06
	R^2	0.9713	0.9560

pH 5, Time 2 h, resin dosage 1 g L⁻¹, concentration of metal ions 25 mg L⁻¹.

ent dosage. As it can be seen from Figure 5(A), two different trends toward the amount of ions adsorption (q) versus the nano-adsorbent dosage were observed. (1) Before the nanoadsorbent dosage 1 (g L⁻¹), an increase in the adsorption of both Cd²⁺ and Ni²⁺ by using the N₂ plasma-treated electrospun PS nanofibrous sample functionalization with AAm [sample (D₂)] was observed; (2) After the nanoadsorbent dosage 1 (g L⁻¹), with raising the dosage, a reduction in the (q) was occurred. The reason of this behavior was referred to levelling down the functionalized groups' accessibility such as either amine or amide on the sample surface for adsorbing the ions because of the active sites unsaturation in which the ions were not able to fulfil completely them during the adsorption process during time of 2 h. It can be concluded that with increasing the nanoadsorbent dosages from 0.5 to 5 g L⁻¹ the Cd²⁺ and Ni²⁺ removal efficiencies were raised up to 96% and 94%, respectively [Figure 5(b)]. Some similar research works also were explained that by increasing the active sites concentration onto the polymer surface using functionalization or grafting processes, an increase in ions removal efficiency was remarkably achieved.^{4,18,30,51} In other words, removal of heavy metal ions and compounds from contaminated metal effluent using electrospun

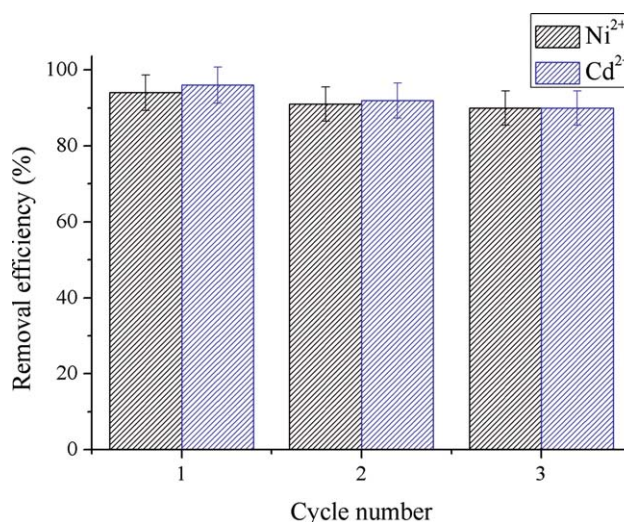


Figure 7. Heavy metal removal efficiency (%R) of the sample as a function of cycle number. [Color figure can be viewed in the online issue, which is available at wileyonlinelibrary.com.]

fibrous membranes is basically originated from the interactions between the heavy metal ions and the functional sites on the surface of nanofibers, such as the physical affinity and electrostatic interactions, or chemical chelating and complexation.²⁰

A simple schematic regarding AAm monomer functionalizing onto the electrospun PS nanofibers and also the adsorption mechanisms of Cd²⁺ in order to provide active sites bindings onto the sample surface is exhibited in Scheme 1. For further investigation of the adsorption type and rearrangement of the active sites provided by AAm functionalization onto the surface of electrospun PS nanofibrous sample, two wellknown isotherm models including Langmuir and Freundlich were applied herein. As known to all, in the Langmuir isotherm, it is sophisticated that there was no reaction through the absorbed molecules as long as all the active sites onto the polymer surface were saturated and occupied.⁵² In other words, the Langmuir model assumes a monolayer coverage of the adsorbate over a homogeneous adsorbent surface and the adsorption of each molecule onto the surface has the same activation energy of adsorption.⁵³ In contrast to the Langmuir model, the Freundlich's isotherm assumes a heterogeneous surface with a nonuniform distribution of heat of adsorption governs throughout the surface with the possibility of multilayer adsorption.^{36,54} The variables of Langmuir and Freundlich's isotherm models can be determined on the basis of experimental data and their kinetic equilibrium adsorptions can be able to discuss in detail according to the linear eqs. (6) and (7), respectively.

$$\frac{1}{q_e} = \frac{1}{q_m} + \frac{1}{K_L q_m} \times \frac{1}{C_e} \quad (6)$$

$$\ln(q_e) = \ln(K_F) + \frac{1}{n} \times \ln(C_e) \quad (7)$$

By the use of the above mentioned equation, the best fit regarding Langmuir and Freundlich's isotherm models with a linear behavior corresponding to the experimental data from AAS analysis was carried out which are represented in Figure 6(a,b). Considering the regression coefficients (R^2) results obtained from the linear Langmuir isotherm [Figure 6(a)] (0.9713 for Cd²⁺, 0.9760 for Ni²⁺) and the linear Freundlich's isotherm model [Figure 6(b)] (0.9990 for Cd²⁺, 0.9998 for Ni²⁺), the sample used in this work followed Freundlich's isotherm model. Table II shows the variables amounts in the Langmuir and Freundlich's isotherm models. As it is clear from this table, 1/n number in Freundlich's isotherm model for both Cd²⁺ and Ni²⁺ ions was about 0.5 and it can be sophisticated that a normal adsorption²⁵ was governed as the main mechanism for removal of the ions via the nanoadsorbent sample. In other words, the adsorption of Cd²⁺ and Ni²⁺ onto the surface of N₂ plasma-modified electrospun PS nanofibrous sample functionalization with AAm was mostly favorable in the aqueous solutions.

Regeneration of the PS nanofibrous adsorbent is important from economical aspect. As shown in Figure 7, removal efficiencies for Ni²⁺ and Cd²⁺ were above 90% in all three cycles and only a reduction of 3–5% was observed.

CONCLUSIONS

The heavy ions metal pollution from various industries in water and aquatic life of mankind owing to its severe toxicity and haz-

ardous side effects is a much more serious issue which encouraged us to carry out this research work. Herein, the electrospun PS nanofibers functionalization with acrylamide using plasma were successfully prepared by using electrospinning technique. Nitrogen plasma treatment by adding AAm was a more suitable method for the creation of amine groups on the samples surfaces compared to mixture of hydrogen and nitrogen as well as ammonia gas plasma treatment. The functionalizing was confirmed by ATR-FTIR analysis, FE-SEM investigation, and WCA measurements. The PS nanofibers prepared according to the optimum conditions exhibited a great ability to adsorb Ni²⁺ and Cd²⁺ ions. The adsorption process was affected by the solution pH and nanoadsorbent dosage. The pH 5 was found to be the optimum value in the process with a desirable correspondence to the Freundlich type of adsorption. The results illustrated that the AAm-PS nanofibers as a cost-effective nanoadsorbent with relatively large adsorption capacity as well as high recyclability was the appropriate alternative to remove heavy metals from water. The PS nanofibers adsorbent in the absorption of cadmium over nickel metal has been shown more efficiency.

REFERENCES

- Hokkanen, S.; Repo, E.; Suopajarvi, T.; Liimatainen, H.; Niinimaa, J.; Sillanpää, M. *Cellulose* **2014**, *21*, 1471.
- Scoullou, M.; Vonkeman, G.; Thornton, I.; Makuch, Z. In *Mercury–Cadmium–Lead Handbook for Sustainable Heavy Metals Policy and Regulation*; Scoullou, M., Ed.; Springer: Netherlands, 2001; Chapter 4.
- Huang, M. R.; Peng, Q. Y.; Li, X. G. *Chem. Eur. J.* **2006**, *12*, 4341.
- Li, X. G.; Liu, R.; Huang, M. R. *Chem. Mater.* **2005**, *17*, 5411.
- Rabuni, M. F.; Nik Sulaiman, N. M.; Awanis Hashim, N. *Desalin. Water Treat.* doi: 10.1080/19443994.2015.1012336, 1 2015.
- Pedersen, K. B.; Kirkelund, G. M.; Ottosen, L. M.; Jensen, P. E.; Lejon, T. *J. Hazard. Mater.* **2015**, *283*, 712.
- Xu, F.; Kim, J. H.; Kim, H. U.; Jang, J. H.; Yook, K. S.; Lee, J. Y.; Hwang, D. H. *Macromolecules* **2014**, *47*, 7397.
- Wang, Z.; Feng, Y.; Hao, X.; Huang, W.; Feng, X. *J. Mater. Chem. A* **2014**, *2*, 10263.
- Karami, H. *Chem. Eng. J.* **2013**, *219*, 209.
- El-Hag Ali, A.; Shawky, H. A.; Abd El Rehim, H. A.; Hegazy, E. A. *Eur. Polym. J.* **2003**, *39*, 2337.
- Yao, Q.; Xie, J.; Liu, J.; Kang, H.; Liu, Y. *J. Polym. Res.* **2014**, *21*, 465.
- Amin, N. K. *Desalination* **2008**, *223*, 152.
- Abdouss, M.; Shoushtari, A. M.; Shamloo, N.; Haji, A. *Polym. Polym. Compos.* **2013**, *21*, 251.
- Jiang, W.; Chen, X.; Pan, B.; Zhang, Q.; Teng, L.; Chen, Y.; Liu, L. *J. Hazard. Mater.* **2014**, *276*, 295.
- Huang, M. R.; Lu, H. J.; Li, X. G. *J. Mater. Chem.* **2012**, *22*, 17685.
- Li, X. G.; Ma, X. L.; Sun, J.; Huang, M. R. *Langmuir* **2009**, *25*, 1675.

17. Li, X. G.; Feng, H.; Huang, M. R. *Chem. Eur. J.* **2009**, *15*, 4573.
18. Lü, Q. F.; Huang, M. R.; Li, X. G. *Chem. Eur. J.* **2007**, *13*, 6009.
19. Dharanivasan, G.; Rajamuthuramalingam, T.; Michael Immanuel Jesse, D.; Rajendiran, N.; Kathiravan, K. *Appl. Nanosci.* **2015**, *5*, 39.
20. Huang, Y.; Miao, Y. E.; Liu, T. *J. Appl. Polym. Sci.* doi: 10.1002/app.408642014.
21. Leonor, I. B.; Kim, H. M.; Balas, F.; Kawashita, M.; Reis, R. L.; Kokubo, T.; Nakamura, T. *J. Mater. Sci. Mater. Med.* **2007**, *18*, 1923.
22. Shin, D. H.; Ko, Y. G.; Choi, U. S.; Kim, W. N. *Ind. Eng. Chem. Res.* **2004**, *43*, 2060.
23. Bulbul Sonmez, H.; Senkal, B. F.; Sherrington, D. C.; Bıcak, N. *React. Funct. Polym.* **2003**, *55*, 1.
24. Reddy, A. R.; Reddy, K. H. *J. Chem. Sci.* **2003**, *115*, 155.
25. Masoumi, A.; Hemati, K.; Ghaemy, M. *RSC Adv.* doi: 10.1039/C4RA10830B2014.
26. Saadeh, H. A.; Abu Shairah, E. A.; Charef, N.; Mubarak, M. S. *J. Appl. Polym. Sci.* **2012**, *124*, 2717.
27. Arslan, M.; Yiğitoğlu, M. *J. Appl. Polym. Sci.* **2008**, *110*, 30.
28. Awokoya, K.; Moronkola, B.; Chigome, S.; Ondigo, D.; Tshentu, Z.; Torto, N. *J. Polym. Res.* **2013**, *20*, 1.
29. Chen, D.; Miao, Y. E.; Liu, T. *ACS Appl. Mater. Inter.* **2013**, *5*, 1206.
30. Feng, S. Q.; Shen, X. Y. *J. Macromol. Sci. B* **2011**, *50*, 1673.
31. Najafabadi, H. H.; Irani, M.; Roshanfekar-Rad, L.; Heydari-Haratameh, A.; Haririan, I. *RSC Adv.* **2015**, *5*, 16532.
32. Khorasani, M. T.; Mirzadeh, H. *J. Biomater. Sci. Polym. E.* **2004**, *15*, 59.
33. Abenojar, J.; Torregrosa-Coque, R.; Martínez, M. A.; Martín-Martínez, J. M. *Surf. Coat. Technol.* **2009**, *203*, 2173.
34. Kalapat, N.; Amornsakchai, T. *Surf. Coat. Technol.* **2012**, *207*, 594.
35. Larrieu, J.; Held, B.; Clément, F.; Hiorns, R. C. *Eur. Phys. J. Appl. Phys.* **2003**, *22*, 61.
36. Haji, A.; Mousavi Shoushtari, A.; Abdouss, M. *Desalin. Water Treat.* **2013**, *53*, 3632.
37. Wang, M. J.; Chang, Y. I.; Poncin-Epaillard, F. *Surf. Interface Anal.* **2005**, *37*, 348.
38. Paynter, R. W. *Surf. Interface Anal.* **1998**, *26*, 674.
39. Boulares-Pender, A.; Prager-Duschke, A.; Elsner, C.; Buchmeiser, M. R. *J. Appl. Polym. Sci.* **2009**, *112*, 2701.
40. Chan, C. M.; Ko, T. M.; Hiraoka, H. *Surf. Sci. Rep.* **1996**, *24*, 1.
41. Motealleh, B.; Zahedi, P.; Rezaeian, I.; Moghimi, M.; Abdolghaffari, A. H.; Zarandi, M. A. *J. Biomed. Mater. Res. B: Appl. Biomater.* **2014**, *102*, 977.
42. Popelka, A.; Kronek, J.; Novák, I.; Kleinová, A.; Mičušík, M.; Špírková, M.; Omastová, M. *Vacuum* **2014**, *100*, 53.
43. Wu, S.; Shanks, R. A. *J. Appl. Polym. Sci.* **2004**, *93*, 1493.
44. Nie, F. Q.; Xu, Z. K.; Yang, Q.; Wu, J.; Wan, L. S. *J. Membr. Sci.* **2004**, *235*, 147.
45. Vanderborght, M.; Van Grieken, E. *Anal. Chem.* **1977**, *49*, 311.
46. Saeed, K.; Haider, S.; Oh, T. J.; Park, S. Y. *J. Membr. Sci.* **2008**, *322*, 400.
47. Vuković, G. D.; Marinković, A. D.; Čolić, M.; Ristić, M. Đ.; Aleksić, R.; Perić-Grujić, A. A.; Uskoković, P. S. *Chem. Eng. J.* **2010**, *157*, 238.
48. Zhao, J.; Geuskens, G. *Eur. Polym. J.* **1999**, *35*, 2115.
49. Güçlü, G.; Güçlü, K.; Keleş, S. *J. Appl. Polym. Sci.* **2007**, *106*, 1800.
50. Haji, A.; Abdouss, M.; Shoushtari, A. M. in 11th World Filtration Congress, Graz, Austria: **2012**, p 1.
51. Shanmugapriya, A.; Srividhya, A.; Ramya, R.; Sudha, P. *Int. J. Environ. Sci.* **2011**, *1*, 2086.
52. Ho, Y. S.; Porter, J. F.; McKay, G. *Water Air Soil Poll.* **2002**, *141*, 1.
53. Zargarán, M.; Shoushtari, A. M.; Abdouss, M. *J. Appl. Polym. Sci.* **2010**, *118*, 135.
54. Haji, A.; Mahmoodi, N. M. *Desalin. Water Treat.* **2012**, *44*, 237.